Electrochemistry

DOI: 10.1002/ange.200802749

Promotional Effect of Palladium on the Hydrogen Oxidation Reaction at a PtPd Alloy Electrode**

*Sung Jong Yoo, Hee-Young Park, Tae-Yeol Jeon, In-Su Park, Yong-Hun Cho, and Yung-Eun Sung**

The hydrogen oxidation reaction (HOR) is of central importance in electrochemistry and plays a pivotal role in low-emission energy conversion devices such as for stationary and portable applications.[1–3] Despite its importance, a detailed knowledge of the mechanism of its electrocatalytic performance has been lacking so far. Recently, there have been studies concerning the correlation between the electronic structure and catalytic activity of metals for the HOR.[4,5] The absorption energy of hydrogen is proportional to the hydrogen–metal bond strength and relative level of the position of the d-band center, the density of states, or the d-band vacancy at the Fermi level.[6] Although these factors are pivotal for the kinetics of the HOR, direct experimental inspection of the contributions of these factors has rarely been investigated in electrochemical oxidation of hydrogen.

There are more than enough signs that Pd catalysts have many of the desired electrocatalytic properties for the HOR/hydrogen evolution reaction (HER), since the electron transfer from the Pd surface into the antibonding orbital of the hydrogen molecule plays an important role in breaking the hydrogen bonds, and this process lowers the associated activation energy.[7,8] It was proposed that the major factor involved in the catalytic activity is the electronic structure of the transition metal.[9] More recently, Pandelov and Stimming found enhancement of the HER on Pd/Au(111) electrode surfaces.[10] This result allowed us to determine critical ensembles for hydrogen adsorption and evolution on Pd/Au(111) electrode surfaces, which show distinct differences in their chemical properties relative to bulk Au(111) or Pd monolayer-covered Au(111) electrodes. The enhanced hydrogen evolution was explained by the coverage effect and proton spillover effect. Marković et al. first reported an enhanced HOR/HER at an epitaxial Pd layer on a Pt(111) electrode by elucidating the energetic effect and surface defects.[11] However, there was not enough evidence to manifest these phenomenological correlations between the physical–chemical properties and the catalytic activity.

Herein, we investigated the oxidation of hydrogen at PtPd alloy electrodes of various compositions compared with that obtained at a pure Pt electrode by using an in situ X-ray absorption near-edge structure (XANES) system for conducting gas-phase experiments to analyze the electronic states. We focused on the electronic structures of the PtPd alloys in a hydrogen ambient for the HOR. To clarify these effects, we introduced a correlation between the d-band vacancies of Pt induced by its alloying to form $PtPdH_x$ and the HOR activity. The results unambiguously indicate that PdH_x (Pd spontaneously adsorbed hydrogen gas) causes the electronic structure of Pt to be favorable for the HOR.

Mass-transfer-corrected Tafel plots of the PtPd alloy electrodes are shown in Figure 1. The slope of the Tafel plot is useful to obtain mechanistic information about the HOR.[11,12] The mechanism for the HOR on a polycrystalline Pt electrode

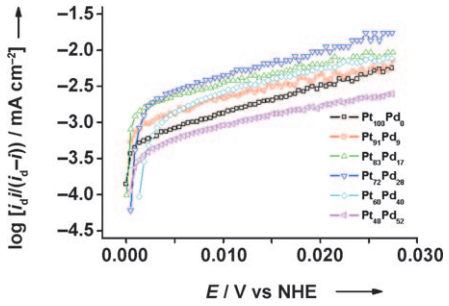

Figure 1. Mass-transfer-corrected Tafel plots for hydrogen oxidation on PtPd alloy electrodes with various compositions in a solution of 0.5 M H_2SO_4. These plots were obtained from Figure S1 in the Supporting Information.

in aqueous electrolyte is considered. This process is usually assumed to proceed by the initial adsorption of hydrogen. This involves an electrochemical adsorption step, in which hydrogen molecule is dissociated (rate-determining step, RDS), followed by an adsorbed hydrogen atom discharge step (fast charge-transfer step), as described in Equations (1)–(3).

$$H_2 \rightarrow H_{ad} + H_{ad} \text{ (Tafel)} \quad (1)$$

$$H_2 \rightarrow H^+ + H_{ad} + e^- \text{ (Heyrovsky)} \quad (2)$$

$$H_2 \rightleftharpoons 2H^+ + 2e^- \text{ (Volmer)} \quad (3)$$

[*] S. J. Yoo, H.-Y. Park, T.-Y. Jeon, I.-S. Park, Y.-H. Cho, Prof. Y.-E. Sung
School of Chemical and Biological Engineering
Seoul National University
Shinlimdong 56-1, Seoul 151-742 (Korea)
Fax: (+82) 2 888 1604
E-mail: ysung@snu.ac.kr

[**] This work was supported in part by KRF (KRF-2006-005J04601), and in part by the Research Center for Energy Conversion and Storage (Contract No. R11-2002-102-00000-0). We are grateful to the Pohang Light Source (PLS) for allowing us to conduct our XAS measurements at their facility.

Supporting information for this article is available on the WWW under http://dx.doi.org/10.1002/anie.200802749.

In the potential range $0.05\ V > E > 0.2\ V$, the Tafel slopes for the PtPd alloy electrodes were approximately 30 mV per decade (Table S1 in the Supporting Information), which is coincident with that (28 mV per decade) of Pt reported by Marković et al.[13] From these results it is reasonable to propose that the HOR takes place on PtPd by the Tafel–Volmer (or Heyrovsky–Volmer) mechanism. Although a number of open questions still remain with regard to the RDS of the electrochemical oxidation of hydrogen in the electrolyte solution, this result indicates that the RDS on the PtPd alloy electrodes is the same as that on a pure Pt electrode.

Figure 2 shows the Arrhenius plots ($\log(i_0)$ versus $1/T$) for the PtPd alloy electrodes. These plots yield straight lines with the slope equal to $-E_a/(2.3\,R)$. The HOR activation energy on $Pt_{72}Pd_{28}$ was much higher than that on Pt. A significant

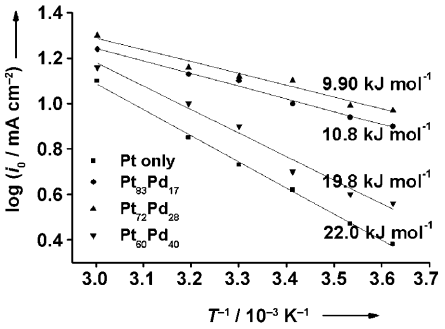

Figure 2. Arrhenius plots of the exchange current densities (i_0) for the PtPd alloy electrodes with various compositions. The activation energy was calculated from the slope, which is equal to $-E_a/(2.3\,R)$.

increase in the kinetic activation energy of the HOR was also observed when the temperature was increased, and the lowest activation energy (9.90 kJ mol^{-1}) was observed on the $Pt_{72}Pd_{28}$ electrode along with a much smaller temperature effect. The $Pt_{60}Pd_{40}$ and Pt electrodes exhibited the highest activation energies of 19.8 and 22.0 kJ mol^{-1} along with much larger temperature effects than those of $Pt_{72}Pd_{28}$ and $Pt_{83}Pd_{17}$, respectively. The activation energies of the $Pt_{60}Pd_{40}$ and Pt electrodes are nearly twice that of $Pt_{72}Pd_{28}$, so it is clear that the activation energy plays an important role in the HOR performance on these materials.

The volcano curve trend in the relationship between the exchange current density and the degree of alloying (Figure 3) indicates that two factors (electronic effect and lattice effect) may influence the alloying effect. First of all, the mechanism for hydrogen intercalation on a Pd electrode in aqueous electrolyte is considered. Hydrogen is a chemically (or electrochemically) reactive gas that adsorbs dissociatively on the Pd surface. Owing to its small size and lower cohesive energy on Pd than on Pt (Pt (564 kJ mol^{-1}) > Pd (376 kJ mol^{-1})),[14] hydrogen can intercalate on a Pd surface and this can lead to strong perturbations of the electronic structure of the Pd surface, which results only in the relaxation of the surface lattice. The absorption of hydrogen on a Pd electrode also leads to modification of the electronic structure of Pd: hydrogen induces electron states below the

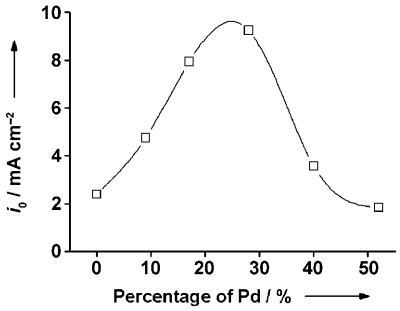

Figure 3. Relationship between the exchange current density and the degree of alloying of PtPd. The exchange current density was measured from the Tafel plots obtained in a solution of 0.5 M H_2SO_4, and the activation energies were calculated from the Arrhenius plots (see Figure 2).

Fermi level and the d-band width is reduced; the d band decreases relative to the Fermi level as the hydrogen concentration increases, which results in a drastic reduction of the density of states (DOS) near the Fermi level.[8] Therefore, Pd undergoes surface reconstruction, which leads to the absorption of hydrogen into its bulk structure. Figure S2 in the Supporting Information shows a reconstruction of the Pd surface and bulk; the transition state is a mixture of α and β phases. The α phase is formed at a low hydrogen gas pressure and the β phase is formed at a high hydrogen gas pressure at potentials near the equilibrium potential by an exothermic reaction. The lattice expansion of $Pt_{72}Pd_{28}H_x$ was observed by measuring the XRD patterns with and without hydrogen (Figure S3 in the Supporting Information). Also, the presence of hydrogen intercalation on the $Pt_{72}Pd_{28}$ electrode in 0.5 M H_2SO_4 electrolyte is shown in Figure S4 in the Supporting Information. Bennet and Gelatt Jr. observed a decrease in the number of unoccupied Pd 4d states in Pd-absorbed hydrogen and narrowing of the d-band width caused by the lattice expansion and modification of the electronic structure.[15] This result shows that the relationship between the HOR and the electronic structure of Pt is affected by PdH_x, assuming that the HOR occurs mainly on the Pt surface, since the exchange current density of pure Pt is higher than that of pure Pd for the HOR in the low overpotential region.

We measured the Pt L_{III} and L_{II} edges using an in situ XANES cell for gas-phase experiments to confirm that the relationship between the HOR and the electronic structure of Pt is affected by the content of hydrogen in PdH_x. One significant aspect of XANES analysis is that it can provide important information on the Pt d-band vacancy. The d-band vacancy is derived from analysis of the Pt L_{III} and L_{II} white lines. The L_{II} and L_{III} edges are due to the excitation of the $2p_{1/2}$ and $2p_{3/2}$ electrons, respectively. These electrons can undergo transitions to empty states in the vicinity of the Fermi level. Since the dipole selection rules in the XANES region restrict the transition to $L = 1$ and $J = 0, 1$ (where L and J are the orbital angular and total angular quantum numbers, respectively), the transitions to the d orbitals are strongly favored.[16] For Pt, it has been shown that the final states with $J = 5/2$ contribute 14 times more than those with $J = 3/2$. The

L_{III} transition ($2p_{3/2}$ to $5d_{5/2}$) is thus more highly favored,[17] by the selection rules, than the L_{II} transition ($2p_{3/2}$ to $5d_{5/2}$). The intensity of the L_{III} peaks and to a lesser extent the L_{II} peaks increases with increasing Pt d-band vacancy.

In general, for hydrogen dissociation, the strong binding of hydrogen would be thought to imply a low hydrogen activation energy barrier.[18] When hydrogen is absorbed onto a Pt metal surface, the σ (bonding) electrons of hydrogen form a coordinate covalent bond, which is shared with the Pt d-band vacancy. At the same time, the Pt d-band orbital lobes overlap the empty hydrogen σ* (antibonding) orbital to undergo back bonding, which strengthens the adsorptive bond between Pt and the head hydrogen atom and weakens the bond between the two hydrogen atoms. Then how is the d-band vacancy related to the adsorptive bond strength of hydrogen? The large vacancy of the Pt d band means that the DOS of Pt is pushed from below the Fermi level to just above the metal Pt valence band, which narrows the d-band width and shifts the d-band center upwards in energy towards the Fermi level, as shown in Figure 4. Greeley et al. showed the

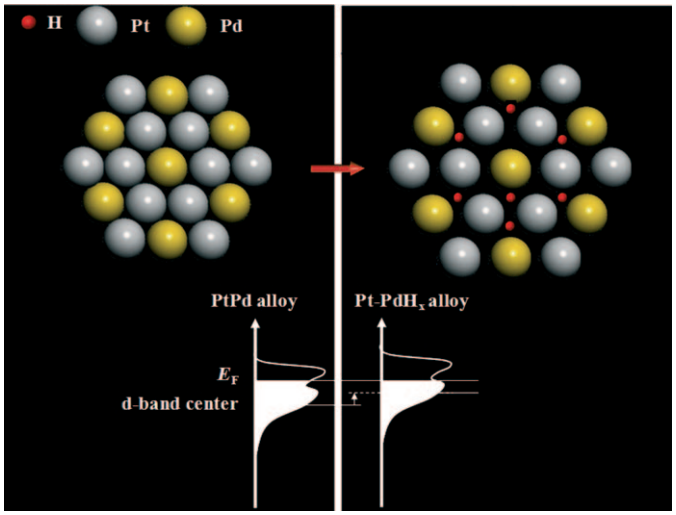

Figure 4. Schematic explanation of the $PtPdH_x$ alloying effect on the d-band state of Pt.

correlation of the d-band states (d-band center) and the free energy of hydrogen adsorption (adsorptive bond strength of hydrogen), and concluded that the upshift of the d-band center leads to a decrease of the hydrogen absorption energy.[5] These concepts are also consistent with those of Nørskov and co-workers who elucidated the coupling between bandwidth and d-band center for the near surface alloys.[19] Therefore, this supposes that larger vacancy of the Pt d band results in stronger adsorptive bond strength of hydrogen.

Figure S5 in the Supporting Information shows the in situ XANES spectra with or without hydrogen on the PtPd alloy electrodes, which were used for calculating the number of d-band vacancies from the Pt L_{III} and L_{II} edge spectra. The peak intensity of the Pt L_{III} and L_{II} edge XANES spectra with hydrogen was shown to be more sensitive to the unoccupied d state than that of the spectra without hydrogen. Since the electronegativity of Pt (2.28) is roughly the same as that of Pd (2.20), no significant charge transfer is to be expected and, hence, the change in the number of d-band vacancies of Pt without hydrogen should be small. In contrast, after charging with hydrogen, the DOS of Pt was significantly modified by the Pd-adsorbed hydrogen.

Figure S6 in the Supporting Information shows the calculations of the d-band vacancy of Pt as a function of the degree of alloying. From the difference in the areas under the Pt L_{III} and L_{II} absorption edges between the sample (pure Pt and PtPd alloys) and a Pt reference foil, the fractional change in the number of d-band vacancies relative to the reference material (f_d) was estimated.[20] This technique therefore constitutes a new way of examining the role of the alloying element in Pt alloys in the d-band vacancy of Pt and, hence, is used in this investigation to elucidate the differences in the degree of electrocatalysis on the Pt versus PtPd alloy electrocatalysts. The number of d-band vacancies of Pt in air ambient decreases as the percentage of Pd increases (Figure S6a), and the number of d-band vacancies of Pt in hydrogen ambient increases as the percentage of Pd increases (Figure S6b). This result means that the d-band width of Pt is increased by the d–d hybridization of Pt and Pd in air ambient and that the d-band center of Pt is downshifted. In contrast, the d-band width of Pt is decreased by the hydrogenation of Pd and the d-band center of Pt is upshifted. These concepts are consistent with those of Nørskov et al. who also elucidated the coupling between the d-band width and d-band center for near surface alloys.[6b,c]

The measurement of the d-band vacancies allows us to correlate directly the catalytic activity for the HOR. As shown in Figure 5, the d-band vacancies of Pt versus the exchange current density exhibits a volcano curve. This result means that the activity of the HOR is given by the strength of the hydrogen–Pt bond interaction, which depends on the position of the Pt d-band states relative to the Fermi level. However, if the number of d-band vacancies of Pt becomes too high, the hydrogen oxidation currents decrease, owing to the stronger adsorptive bond strength of hydrogen, which increases the desorption energy barrier in the charge-transfer step (Volmer reaction). This situation leads to a maximum in the catalytic activity when the ability of the PtPd alloy to bind hydrogen is not too weak and not too strong.

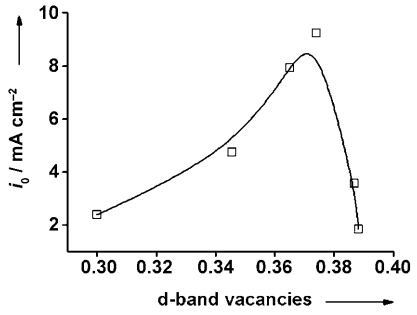

Figure 5. Correlation between exchange current density and d-band vacancies from the in situ XANES data measured after charging with hydrogen.

In conclusion, we found that significant electrocatalysis occurred for the HOR at the PtPd alloy electrodes to an extent that depends on the alloy composition and revealed the principal role of the electronic effect of PtPd alloys in the HOR. We demonstrated that the relationship between the exchange current density and the degree of PtPd alloying exhibits a volcano-shaped trend and that, at the same temperature, the maximum exchange current density for the hydrogen oxidation is obtained at $Pt_{72}Pd_{28}$, which is similar to the trend of the activation energies. We also showed that there is a relationship between the number of d-band vacancies of Pt on the $PtPdH_x$ alloy electrodes as a function of the degree of alloying and the activity of the HOR. Our results imply that the high performance of the $PtPdH_x$ catalyst for the HOR relies heavily on the electronic structure of Pt caused by hydrogen gas spontaneously adsorbed on Pd in the electrocatalytic process.

Experimental Section

PtPd alloy electrodes were grown by using an RF magnetron co-sputtering system consisted of a dual sputtering gun.[21] Si(100) and glassy carbon were used as substrates to characterize the structural and electrochemical properties, respectively. Co-sputtering was performed under an inert Ar gas at a flow rate of 26 sccm at room temperature for 10 min, which produced films about 100 nm thick. To fabricate the PtPd thin film electrodes with various compositions, the guns with the metal targets in the RF magnetron sputtering system were controlled as a function of the RF power. With increasing RF power of the Pd target gun at a fixed RF power of the Pt gun, the Pd concentration was varied from 0 to 52.2%. A pure Pt electrode was also produced. X-ray diffraction (XRD) (MAC Science M18XHF-SRA equipped with a $Cu_{K\alpha}$ source at 30 kV–30 mA) analyses of the as-prepared electrodes were used to determine the degree of crystallinity. To analyze and compare the surface chemical states of the samples, X-ray photoelectron spectroscopy (XPS) was carried out by using a KARATOS (AXIS 165) instrument. The binding energies of Pt and Pd were calibrated with respect to the binding energy of the carbon 1s orbital. The X-ray source was Al Kα with an excitation energy of 1486.6 eV operating at 160 kV/150 W and the base pressure was 1×10^{-9} Torr. The Pt L_{III} edge and Pt L_{II} edge X-ray absorption spectra were recorded on the 7C beam line at the Pohang Light Source (PLS) with a ring current of 120–170 mA at 2.5 GeV.

An AutoLab PGSTAT20 potentiostat and rotating disk electrode (RDE) system (Ecochemie) with a conventional three-electrode configuration were used for all of the electrochemical measurements. All of the electrochemical measurements, except for the HOR with the RDE configuration, were performed in Ar-purged 0.5 M sulfuric acid solution. For the HOR experiment, 99.99% hydrogen gas was bubbled into the electrolyte for 10 min before each measurement. A catalyst-coated glassy carbon electrode with a diameter of 5 mm was used as the working electrode. Before each measurement, the glassy carbon electrode was polished with 0.05 μm alumina paste and washed with deionized water in an ultrasonic bath. A saturated calomel electrode (SCE) with 3 M KCl (Gamry) and glassy carbon rod were used as the reference and counter electrodes, respectively. However, in this paper, all of the potentials were reported with respect to the NHE.

Received: June 11, 2008
Revised: July 31, 2008
Published online: October 29, 2008

Keywords: electrochemistry · fuel cells · hydrogen oxidation · palladium · platinum

[1] a) *Handbook of Fuel Cells: Fundamentals, Technology and Applications* (Eds.: W. Vielstich, A. Lamm, H. Gasteiger), Wiley, Chichester, **2003**; b) C. Y. Wang, *Chem. Rev.* **2004**, *104*, 4727 – 4766.
[2] a) S. Srinivasan, D. J. Manko, H. Koch, M. A. Enayetullah, A. J. Appleby, *J. Power Sources* **1990**, *29*, 367 – 387; b) T. E. Springer, T. A. Zawodzinski, S. Gottesfeld, *J. Electrochem. Soc.* **1991**, *138*, 2334 – 2342; c) L. Carrette, K. A. Friedrich, U. Stimming, *Fuel Cells* **2001**, *1*, 5 – 39; d) C. K. Dyer, *J. Power Sources* **2002**, *106*, 31 – 34.
[3] a) B. C. H. Steele, A. Heinzel, *Nature* **2001**, *414*, 345 – 352; b) K.-W. Park, Y.-E. Sung, *J. Ind. Eng. Chem.* **2006**, *12*, 165 – 174.
[4] a) S. Mukerjee, J. McBreen, *J. Electroanal. Chem.* **1998**, *448*, 163 – 171; b) K. Sasaki, Y. Mo, J. X. Wang, M. Balasubramanian, F. Uribe, J. McBreen, R. R. Adzic, *Electrochim. Acta* **2003**, *48*, 3841 – 3849.
[5] a) J. Greeley, M. Mavrikakis, *Nat. Mater.* **2004**, *3*, 810 – 815; b) J. Greeley, J. K. Nørskov, L. A. Kibler, A. M. El-Aziz, D. M. Kolb, *ChemPhysChem* **2006**, *7*, 1032 – 1035.
[6] a) B. E. Conway, E. M. Beatty, P. A. D. DeMaine, *Electrochim. Acta* **1962**, *7*, 39; b) J. K. Nørskov, T. Bligaard, A. Logadottir, J. R. Kitchin, J. G. Chen, S. Pandelov, U. Stimming, *J. Electrochem. Soc.* **2005**, *152*, J 23 – J26; c) T. Bligaard, J. K. Nørskov, *Electrochim. Acta* **2007**, *52*, 5512 – 5516.
[7] F. A. Lewis, *The Palladium Hydrogen System*, Academic, New York, **1967**.
[8] a) P. A. Bennett, J. C. Fuggle, *Phys. Rev. B* **1982**, *26*, 6030 – 6039; b) S. Mizusaki, T. Miyatake, N. Sato, I. Yamamoto, M. Yamaguchi, M. Itou, Y. Sakurai, *Phys. Rev. B* **2006**, *73*, 113101; c) J. H. Weaver, *Phys. Rev. B* **1975**, *11*, 1416 – 1425.
[9] a) J. Greeley, J. K. Nørskov, M. Mavrikakis, *Annu. Rev. Phys. Chem.* **2002**, *53*, 319 – 348; b) J. A. Rodriguez, D. W. Goodman, *Science* **1992**, *257*, 897 – 903; c) F. Maroun, F. Ozanam, O. M. Magnussen, R. J. Behm, *Science* **2001**, *293*, 1811 – 1814.
[10] S. Pandelov, U. Stimming, *Electrochim. Acta* **2007**, *52*, 5548 – 555.
[11] N. M. Markovic, C. A. Lucas, V. Climent, V. Stamenkovi, P. N. Ross, *Surf. Sci.* **2000**, *465*, 103 – 114.
[12] H. A. Gasteiger, N. M. Markovic, P. N. Ross, *J. Phys. Chem.* **1995**, *99*, 8290 – 8301.
[13] N. M. Markovic, B. N. Grgur, P. N. Ross, *J. Phys. Chem. B* **1997**, *101*, 5405 – 5413.
[14] *CRC Handbook of Chemistry and Physics* (Ed.: D. R. Lide) 85th ed., CRC, Boca Raton, FL, **2004**.
[15] a) C. D. Gelatt, Jr., H. Ehrenreich, J. A. Weiss, *Phys. Rev. B* **1978**, *17*, 1940 – 1957; b) P. A. Bennett, J. C. Fuggle, *Phys. Rev. B* **1982**, *26*, 6030 – 6039.
[16] L. M. Falicov, W. Hanke, M. P. Maple, *Valence Fluctuation in Solids*, North-Holland, Amsterdam, **1981**.
[17] A. E. Russell, S. Maniguet, R. J. Mathew, J. Yao, M. A. Roberts, D. Thompsett, *J. Power Sources* **2001**, *96*, 226 – 232.
[18] a) J. K. Nørskov, T. Bligaarda, A. Logadottira, S. Bahna, L. B. Hansena, M. Bollingera, H. Bengaarda, B. Hammerb, Z. Sljivancaninb, M. Mavrikakisc, Y. Xuc, S. Dahld, C. J. H. Jacobsend, *J. Catal.* **2002**, *209*, 275 – 278; b) Y. Xu, A. V. Ruban, M. Mavrikakis, *J. Am. Chem. Soc.* **2004**, *126*, 4717 – 4725; c) A. Michaelides, Z.-P. Liu, C. J. Zhang, A. Alavi, D. A. King, P. Hu, *J. Am. Chem. Soc.* **2003**, *125*, 3704 – 3705.
[19] J. R. Kitchin, J. K. Nørskov, M. A. Barteau, J. G. Chen, *J. Chem. Phys.* **2004**, *120*, 10240 – 10246.
[20] A. N. Mansour, J. W. Cook, D. E. Sayers, *J. Phys. Chem.* **1984**, *88*, 330 – 2334.
[21] K.-W. Park, J.-H. Choi, K.-S. Ahn, Y.-E. Sung, *J. Phys. Chem. B* **2004**, *108*, 5989 – 5994.

